Impulse Response of Anisotropic Composite Plates with a Higher-Order Theory and Finite Element Discretization

Tarun Kant, Mallikarjuna
Indian Institute of Technology, Bombay, India

INTRODUCTION

The global safety of nuclear power plants is greatly affected by the resistance of internal and external plate and shell-type structures to dynamic loads caused by accidentally generated flying objects, such as parts of failed rotating equipment or ruptured piping, tornado missiles or impacting aircraft engines. This paper describes the development of a linear and nonlinear laminated plate dynamics computer program based on explicit time integration with a special mass matrix diagonalization scheme using a higher-order theory and C^0 finite elements. A Lagrangian approach is adopted for the geometric nonlinear analysis and the stress and strain descriptions used are those due to Piola-Kirchhoff and Green respectively.

GEOMETRICALLY NONLINEAR HIGHER-ORDER THEORY

In the case of fibre-reinforced composite materials, a laminated theory which takes into account the effects of transverse shear deformation and rotary inertia is in general required. A laminate with constant thickness, h, composed of NL orthotropic layers oriented at angles $\alpha_1, \alpha_2, \ldots, \alpha_{NL}$ is considered. The origin of the co-ordinate system is licated within the middle plane (x-y) with the z-axis being normal of the midplane. The higher-order theory is based on the following assumed displacement field,

$$
\begin{aligned}
u(x,y,z,t) &= u_o(x,y,t) + z\theta_x(x,y,t) + z^3\theta_x^*(x,y,t) \\
v(x,y,z,t) &= v_o(x,y,t) + z\theta_y(x,y,t) + z^3\theta_y^*(x,y,t) \\
w(x,y,z,t) &= w_o(x,y,t) \qquad \ldots (1a)
\end{aligned}
$$

with midplane displacement vector,

$$\underset{\sim}{d} = (u_o, v_o, w_o, \theta_x, \theta_y, \theta_x^*, \theta_y^*)^t \qquad \ldots (1b)$$

Introducing the Von Karman assumptions which imply that derivatives of u and v with respect to x, y, and z are small and noting that w is independent of z allows Green's strain to be written as follows:

$$\underset{\sim}{\varepsilon} = \begin{bmatrix} \varepsilon_x \\ \varepsilon_y \\ \gamma_{xy} \\ \gamma_{yz} \\ \gamma_{zx} \end{bmatrix} = \begin{bmatrix} \partial u/\partial x + 0.5\,(\partial w/\partial x)^2 \\ \partial v/\partial y + 0.5\,(\partial w/\partial y)^2 \\ \partial u/\partial y + \partial v/\partial x + (\partial w/\partial x)(\partial w/\partial y) \\ \partial v/\partial z + \partial w/\partial y \\ \partial u/\partial z + \partial w/\partial x \end{bmatrix} \quad \ldots (2)$$

The expressions for Piola-Kirchhoff stresses in the L^{th} layer can be written by substitution of the Green strain expressions as follows:

$$\begin{bmatrix} \sigma_x \\ \sigma_y \\ \tau_{xy} \\ \tau_{yz} \\ \tau_{zx} \end{bmatrix}^L = \begin{bmatrix} Q_{11} & Q_{12} & Q_{13} & 0 & 0 \\ & Q_{22} & Q_{23} & 0 & 0 \\ & & Q_{33} & 0 & 0 \\ & & & Q_{44} & Q_{45} \\ \text{Symmetric} & & & & Q_{55} \end{bmatrix}^L \begin{bmatrix} \varepsilon_{x_o} + z\chi_x + z^3\chi_x^* + 0.5(\partial w_o/\partial x)^2 \\ \varepsilon_{y_o} + z\chi_y + z^3\chi_y^* + 0.5(\partial w_o/\partial y)^2 \\ \varepsilon_{xy_o} + z\chi_{xy} + z^3\chi_{xy}^* + (\partial w_o/\partial x)\,(\partial w_o/\partial y) \\ \Phi_y + \Phi_y^* \\ \Phi_x + \Phi_x^* \end{bmatrix} \quad \ldots (3a)$$

in which,

$$(\varepsilon_{x_o}, \varepsilon_{y_o}, \varepsilon_{xy_o}, \chi_x, \chi_y, \chi_{xy}) = \left(\frac{\partial u_o}{\partial x}, \frac{\partial v_o}{\partial y}, \frac{\partial u_o}{\partial y} + \frac{\partial v_o}{\partial x}, \frac{\partial \theta_x}{\partial x}, \frac{\partial \theta_y}{\partial y}, \frac{\partial \theta_x}{\partial y} + \frac{\partial \theta_y}{\partial x}\right)$$

$$(\chi_x^*, \chi_y^*, \chi_{xy}^*, \Phi_x, \Phi_y, \Phi_x^*, \Phi_y^*) = \left(\frac{\partial \theta_x^*}{\partial x}, \frac{\partial \theta_y^*}{\partial y}, \frac{\partial \theta_x^*}{\partial y} + \frac{\partial \theta_y^*}{\partial x}, \theta_x + \frac{\partial w_o}{\partial x}, \theta_y + \frac{\partial w_o}{\partial y}, 3\theta_x^*, 3\theta_y^*\right) \quad \ldots (3b)$$

and the coefficients of transformed reduced stiffness matrix $\underset{\sim}{Q}$ are given in references (Jones, 1975 or Mallikarjuna, 1989).

The expressions for membrane, flexure and shear stress-resultants are as follows:

$$\begin{bmatrix} N_x, N_y, N_{xy} \\ M_x, M_y, M_{xy} \\ M_x^*, M_y^*, M_{xy}^* \end{bmatrix} = \sum_{L=1}^{NL} \int_{h_{L-1}}^{h_L} \begin{bmatrix} \sigma_x, & \sigma_y, & \tau_{xy} \\ z\sigma_x, & z\sigma_y, & z\tau_{xy} \\ z^3\sigma_x, & z^3\sigma_y, & z^3\tau_{xy} \end{bmatrix}^L dz \quad \ldots (4a)$$

$$\begin{bmatrix} Q_x, & Q_y \\ Q_x^*, & Q_y^* \end{bmatrix} = \sum_{L=1}^{NL} \int_{h_{L-1}}^{h_L} \begin{bmatrix} \tau_{xz}, & \tau_{yz} \\ z^2\tau_{xz}, & z^2\tau_{yz} \end{bmatrix}^L dz \quad \ldots (4b)$$

The integral of Eqns.(4) after substitution of the corresponding stresses from expressions (3) leads to the following constitutive relations for the laminate which is written in a compacted form as,

$$\underset{\sim}{\bar{\sigma}} = \underline{D}\,\underset{\sim}{\bar{\varepsilon}} \quad \ldots (5a)$$

in which $\underset{\sim}{\bar{\sigma}} = (N_x, N_y, N_{xy}, M_x, M_y, M_{xy}, M_x^*, M_y^*, M_{xy}^*, Q_x, Q_y, Q_x^*, Q_y^*)^t$

$$\underset{\sim}{\bar{\varepsilon}} = (\varepsilon_{x_o}+0.5(\partial w_o/\partial x)^2,\ \varepsilon_{y_o}+0.5(\partial w_o/\partial y)^2,\ \varepsilon_{xy_o}+(\partial w_o/\partial x)(\partial w_o/\partial y),$$
$$\chi_x, \chi_y, \chi_{xy}, \chi_x^*, \chi_y^*, \chi_{xy}^*,\ \Phi_x, \Phi_y, \Phi_x^*, \Phi_y^*)^t \qquad \ldots(5b)$$

and the rigidity matrix $\underline{D}$ is written in a concise matrix form as follows:

$$\underline{D} = \begin{bmatrix} \underline{D}_m & \underline{D}_c & \underline{0} \\ \underline{D}_c^t & \underline{D}_b & \underline{0} \\ \underline{0} & \underline{0} & \underline{D}_s \end{bmatrix};$$

D_m = Membrane rigidity
D_b = Flexure rigidity
D_c = Membrane-flexure coupling rigidity
D_s = Shear rigidity ...(5c)

$$D_{m_{ij}} = \sum_{L=1}^{NL} \int_{h_{L-1}}^{h_L} \underline{Q}_{ij}^L \, dz \ ; \quad D_{c_{ij}} = \sum_{L=1}^{NL} \int_{h_{L-1}}^{h_L} \underline{Q}_{ij}^L \begin{bmatrix} z & z^3 \end{bmatrix} dz$$

$$D_{b_{ij}} = \sum_{L=1}^{NL} \int_{h_{L-1}}^{h_L} \underline{Q}_{ij}^L \begin{bmatrix} z^2 & z^4 \\ z^4 & z^6 \end{bmatrix} dz \ ; \quad D_{s_{ij}} = \sum_{L=1}^{NL} \int_{h_{L-1}}^{h_L} \underline{Q}_{\ell m}^L \begin{bmatrix} 1 & z^2 \\ z^2 & z^4 \end{bmatrix} dz$$

$$(i,j = 1,2,3 \ ; \ \ell,m = 5,4) \qquad \ldots(5d)$$

Laminate Strain-Displacement Relations

The variation of total strain (mid-plane strain) $\delta\underset{\sim}{\bar{\varepsilon}}_t$ due to the virtual displacements $\delta\underset{\sim}{d}$ is given as the sum of the variation of the linear (LI) and nonlinear (NL) generalized strain as

$$\delta\underset{\sim}{\bar{\varepsilon}}_t = \delta\underset{\sim}{\bar{\varepsilon}}_{LI} + \delta\underset{\sim}{\bar{\varepsilon}}_{NL} \qquad \ldots(6a)$$

Since $\delta\underset{\sim}{\bar{\varepsilon}}_{LI}$ is a usual linear, infinitesimal strain vector which is a function of $\underset{\sim}{d}$,

$$\delta\underset{\sim}{\bar{\varepsilon}}_{LI} = \underline{L}\,\delta\underset{\sim}{d} \qquad \ldots(6b)$$

where $\underline{L}$ is the normal linear strain-displacement differential operater matrix. If the displacement gradients with respect to the lateral displacement w_o are

$$\underset{\sim}{\theta}_{NL} = (\partial w_o/\partial x,\ \ \partial w_o/\partial y)^t \qquad \ldots(6c)$$

then the variation of the nonlinear component of the inplane strain in terms of the virtual gradients $\delta\underset{\sim}{\theta}_{NL}$ is

$$\delta\underset{\sim}{\varepsilon}_{NL} = \frac{1}{2}\,\delta\underline{A}_\theta\underset{\sim}{\theta}_{NL} + \frac{1}{2}\,\underline{A}_\theta\,\delta\underset{\sim}{\theta}_{NL} \qquad \ldots(6d)$$

$$\delta\underset{\sim}{\varepsilon}_{NL} = \underline{A}_\theta\,\delta\underset{\sim}{\theta}_{NL} \qquad \ldots(6e)$$

where

$$\underline{A}_\theta = \begin{bmatrix} \partial w_o/\partial x & 0 \\ 0 & \partial w_o/\partial y \\ \partial w_o/\partial y & \partial w_o/\partial x \end{bmatrix} \qquad \ldots(6f)$$

FINITE ELEMENT DISCRETIZATION

In the isoparametric C^0 finite element formulation, the same shape functions are used to define the coordinates as well as the displacement of any point on the reference xy-plane of the laminate in terms of their nodal values. Thus, the space (x,y) coordinates are expresses as

$$x = \sum_{i=1}^{NN} N_i(\xi,\eta)\, x_i \quad \text{and} \quad y = \sum_{i=1}^{NN} N_i(\xi,\eta)\, y_i \qquad \ldots (7)$$

and the components of the generalized (mid-plane) displacement vector $\underset{\sim}{d}\,(\xi,\eta,t)$ are expressed as follows by discretizing space (x,y) only commonly termed as partial discretization,

$$\underset{\sim}{d}(\xi,\eta,t) = \sum_{i=1}^{NN} N_i(\xi,\eta)\, \underset{\sim}{d}_i(t) \qquad \ldots (8a)$$

in which 't' is the time, NN is the number of nodes in an element, N_i is the simple isoparametric interpolating function associated with node 'i' in terms of the normalized coordinates ξ and η, and $\underset{\sim}{d}_i(t)$ is the generalized displacement vector corresponding to i^{th} node of an element.

Equation (8a) can also be written as

$$\underset{\sim}{d}(\xi,\eta,t) = \underline{N}(\xi,\eta)\, \underset{\sim}{a}_e(t) \qquad \ldots (8b)$$

where $\underline{N}$ is the shape function matrix and is given by

$$\underline{N} = \left[\underline{N}_1, \underline{N}_2, \ldots, \underline{N}_{NN}\right] \qquad \ldots (8c)$$

and a_e is the element displacement vector and is written as

$$\underset{\sim}{a}_e^t = \left[\underset{\sim}{d}_1^t, \underset{\sim}{d}_2^t, \ldots, \underset{\sim}{d}_{NN}^t\right] \qquad \ldots (8d)$$

Element Stiffness Matrix

The virtual displacements $\delta\underset{\sim}{d}$ are written in terms of the nodal virtual displacements $\delta\underset{\sim}{a}_e$ from Eqn. (8b) as

$$\delta\underset{\sim}{d} = \underline{N}\,\delta\underset{\sim}{a}_e \qquad \ldots (9)$$

The displacement gradients $\underset{\sim}{\theta}_{NL}$ in Eqn. (6c) may now be written in discrete form in terms of the nodal displacements $\underset{\sim}{a}_e$ and Cartesian derivatives of the shape functions as,

$$\underset{\sim}{\theta}_{NL} = \underline{G}\,\underset{\sim}{a}_e \qquad \ldots (10a)$$

where

$$\underline{G} = \underline{G}_1, \underline{G}_2, \ldots, \underline{G}_{NN} \qquad \ldots (10b)$$

and

$$\underline{G}_i = \begin{bmatrix} 0 & 0 & \partial N_i/\partial x & 0 & 0 & 0 & 0 \\ 0 & 0 & \partial N_i/\partial y & 0 & 0 & 0 & 0 \end{bmatrix} \qquad \ldots (10c)$$

The generalized Green's strain vector $\bar{\underset{\sim}{\varepsilon}}_t$ given by Eqn.(6a) is expressed in terms of nodal displacements $\underset{\sim}{a}_e$, displacement gradients $\underline{A}_\theta$ and Cartesian derivatives of $\underline{N}$ as

$$\bar{\underset{\sim}{\varepsilon}}_t = \left[\underline{B}_{LI} + \frac{1}{2}\underline{B}_{NL}(\underset{\sim}{a}_e)\right]\underset{\sim}{a}_e \qquad \ldots (11a)$$

where $\underline{B}_{LI}$ is the strain-displacement matrix giving the linear strains and $\underline{B}_{NL}$, which is linearly dependent upon $\underset{\sim}{a}_e$, giving the nonlinear strains $\underset{\sim}{\varepsilon}_{NL}$. Consequently the nonlinear strains are quadratically dependent upon the nodal displacements $\underset{\sim}{a}_e$,

where
$$\underline{B}_{NL_i} = \begin{bmatrix} \underline{A}_\theta \\ \underline{0} \\ \underline{0} \end{bmatrix} \underline{G}_i \qquad \text{...(11b)}$$

Now, the total tangential stiffness matrix is readily written as,

$$\underline{K}_t^e = \underline{K}_{LI}^e + \underline{K}_{NL}^e + \underline{K}_\sigma^e \qquad \text{...(12a)}$$

where $\underline{K}_{LI}^e$ represents the usual, small displacements stiffness matrix, $\underline{K}_{NL}^e$ is due to large displacement which is quadratically dependent upon displacement $\underset{\sim}{a}_e$,

$$\underline{K}_{NL}^e = \int_A \underline{B}_{LI}^t \, \underline{D} \, \underline{B}_{NL} \, dA + \int_A \underline{B}_{NL}^t \, \underline{D} \, \underline{B}_{NL} \, dA + \int_A \underline{B}_{NL}^t \, \underline{D} \, \underline{B}_{LI} \, dA \qquad \text{...(12b)}$$

and the initial stress matrix (geometric stiffness matrix) is

$$\underline{K}_\sigma^e = \int_A \underline{G}^t \begin{bmatrix} N_x & N_{xy} \\ N_{xy} & N_y \end{bmatrix} \underline{G} \, dA \qquad \text{...(12c)}$$

Element Mass Matrix

The element consistent mass matrix, unfortunately is not diagonal and the essence of the explicit time marching scheme requires it to be diagonalised. For the quadratic elements used here several alternatives were investigated by Hinton et al. and the most efficient one, at present time, appears to be offered by lumping in proportion to the diagonal terms of the original (consistent) mass matrix. In the present investigation this special mass matrix diagonalization scheme which is more sophisticated than a lumped mass matrix is used which is discussed elsewhere (Hinton et al, 1976 and Mallikarjuna, 1989).

Critical Time Step

In the present work, the very popular and easily implemented, explicit central difference scheme is used. During each time step, relatively little computational effort is required, since no stiffness and mass matrices of the complete element assemblage need to be formed, the solution can essentially be carried out on the element level and relatively little high-speed storage is required. Using this scheme, systems of very large order can be solved effectively. Unfortunately the method is conditionally stable and very small time steps are often needed.

If the mass matrix $\underline{M}$ is diagonal and a_i denotes the i^{th} component (element) of the $\underset{\sim}{a}$ vector, then

$$a_i^{n+1} = \left[(\Delta t)^2/M_{ii}\right] \left[-\sum_{j=1}^{m} K_{ij} \, a_j^n + f_i^n\right] - a_i^{n-1} + 2\,a_i^n \qquad \text{...(13)}$$

(Here m denotes the number of nodal variables)

in which Δt is the time step or interval so that we are sampling the displacements at time stations $t_n - \Delta t$, t_n and $t_n + \Delta t$.

The safe estimate of the critical time step length given by Tsui and Tong is valid only for isotropic plates. In the present investigation, after carrying out extensive numerical computations, the emperical relation given by Tsui and Tong is modified to estimate the critical time step length for the transient response of anisotropic composite laminates.

$$\Delta t \leq \Delta t_{cr} = \Delta x \left[\frac{\rho \ (1 - \nu^2)}{E_2 \ R\left\{ 2 + (1-\nu) \ (\pi^2/12) \ (1+1.5 \ (\Delta x/h)^2)\right\}} \right]^{1/2} \qquad \ldots(14)$$

in which $R = E_1/E_2$, Δx is the smallest distance between adjacent nodes in any quadrilateral element used, E_1 and E_2 are the Young's modulii, where subscripts 1 refers to the direction of fibres and 2 refers to the transverse direction.

RESULTS AND DISCUSSION

In order to establish the versatility of the present higher-order shear deformation theory (HOST) in its ability to model both thick and thin composite and sandwich plates, three computer programs, viz.,

HOST5 $(w,\theta_x,\theta_y,\theta_x^*,\theta_y^*)$ for symmetric laminate,

HOST7 $(u,v,w,\theta_x,\theta_y,\theta_x^*,\theta_y^*)$ for unsymmetric laminate, and

NLHOST7 for nonlinear analysis of laminates,

have been developed separately. In addition to the refined theory (HOST), programs were developed for first-order shear deformation theory (FOST) with w,θ_x,θ_y for symmetric laminates (FOST3), u,v,w,θ_x,θ_y for unsymmetric laminates (FOST5) and NLFOST5 for nonlinear analysis of laminates.

It is well known that the shear correction coefficients depend on the lamination scheme and the lamina material properties. But due to lack of well accepted coefficients for finite plates, the transverse shear energy term in FOST is corrected using a multiplier 5/6 for all the materials except for the core of a sandwich plate where a coefficient of unity has been used. The 9-node Lagrangian quadrilateral isoparametric element is used here, with selective numerical integration scheme, based on Gauss-quadrature rules, viz., 3 x 3 for membrane, coupling between membrane and flexure, flexure and inertia terms and 2 x 2 for shear terms in the energy expression. The computations were carried out on CYBER 180/840 Computer at Indian Institute of Technology, Bombay, India. In all of the numerical examples presented herein, zero initial conditions were assumed.

A quarter plate is used for isotropic, 0^o-orthotropic and cross-ply ($0^o/90^o/\ldots..$) laminates, while a full plate is discretized for angle-ply laminates. The parametric effects of time step, mesh size, aspect ratio, side-to-thickness ratio, lamination scheme and material anisotropy on the dynamic response of the laminates have been studied (Mallikarjuna, 1989). A clamped circular plate under a suddenly applied uniformly distributed step (pulse) load is analysed with DATA-1 (see Table 1). As is evident from Figure 1 where the central deflections are plotted against time, the geometric nonlinearity results in a stiffering effect with a reduction of both the amplitude and the period of vibration. The second example is concerned with a 0^o-orthotropic clamped plate (DATA-2), which is infinitely extended in one direction and is modelled, invoking symmetry, by 5 plate bending elements. The variation of centre transverse deflection and bending moment with respect to time is shown in Figure 2 for different magnitudes of pulse load. It is observed that the effect of the geometric nonlinearity in the Von Karman sense is to decrease the amplitude and period of the centre deflection and stress-resultants.

In order to study the effect of uniformly distributed impulsive loads, $q = q_o H(t-t_o)$, where H(t) denotes the heavy side step function and pulse (step) load $q = q_o$, on the transverse deflection, a clamped four-layer ($0^o/90^o/90^o/0^o$)

Table 1. Material Properties

DATA-1	$E = 100$ psi, $\nu = 0.3$, $\rho = 10$ lb-sec^2/cm^4
DATA-2	For face sheets, the assumed ply data based on Hercules ASI/3501-6 graphite/epoxy prepreg system, $E_1 = 13.08 \times 10^6 N/cm^2$, $E_2 = E_3 = 1.06 \times 10^6 N/cm^2$ $G_{12} = G_{13} = 0.6 \times 10^6 N/cm^2$, $G_{23} = 0.39 \times 10^6 N/cm^2$ $\nu_{12} = \nu_{13} = 0.28$, $\nu_{23} = 0.34$, $\rho = 15.8 \times 10^{-6} N\text{-}sec^2/cm^4$ Core material is of U.S. commercial aluminium honeycomb (1/4 inch cell size, 0.003 inch foil) $G_{23} = G_{yz} = 1.772 \times 10^4 N/cm^2$, $G_{13} = G_{xz} = 5.206 \times 10^4 N/cm^2$ $E_3 = E_z = 3.013 \times 10^5 N/cm^2$, $\rho = 0.1009 \times 10^{-5} N\text{-}sec^2/cm^4$
DATA-3	For face sheets (typical graphite/epoxy) $E_1 = 0.12 \times 10^8 N/cm^2$, $E_2 = E_3 = 0.79 \times 10^6 N/cm^2$, $\nu_{12} = \nu_{23} = \nu_{13} = 0.3$, $G_{12} = G_{23} = G_{13} = 0.55 \times 10^6 N/cm^2$, $\rho = 1.58 \times 10^{-5} N\text{-}sec^2/cm^4$. For core material (U.S. Commercial aluminium honeycomb, 1/4 inch cell size, 0.007 inch foil) $G_{yz} = 0.7034 \times 10^4 N/cm^2$, $G_{xz} = 0.1407 \times 10^5 N/cm^2$, $\rho = 0.3415 \times 10^{-6} N\text{-}sec^2/cm^4$

composite square plate is analysed. Each layer is of equal thickness. The material properties given for face sheets in DATA-2 are used here. The variation of the centre deflection with time is presented using HOST5 in Figure 3. From this figure it is seen that as the duration of impulsive force decreases, the maximum centre transverse deflection decreases. Therefore the damping has much less importance in controlling the maximum response of a structure to impulsive loads than for periodic and harmonic loads. The maximum response to an impulsive load will be reached in a very short time, before the damping forces can absorb much energy from the structure.

The next example is concerned with a clamped five-layer unsymmetric composite-sandwich plate (DATA-2) subjected to a suddenly applied uniformly distributed pulse loading. Figure 4 shows the plot of centre deflection versus time. It is noted that the FOST predicts significantly lower values of deflection and period. This is due to consideration of warping effect in the present theory. Since no damping or internal friction is included in the present study the solutions do not decay with time.

An anisotropic composite-sandwich plate (a full plate modelled with 4 x 4 mesh) clamped on all the four sides is analysed for suddenly applied uniformly distributed pulse loading. The elastic material properties (DATA-3) given in Table 1 are used. The thickness of each stiff layer is 0.025 h and core is 0.8 h. Figure 5 shows the variation of centre transverse deflection and normal stress with time for a/h = 10 and 50. The maximum transverse displacement in HOST is about 70 % and 24 % larger compared to that in FOST for a/h = 10 and 50 respectively. The maximum centre normal stress obtained by HOST is about 40 % higher compared to that of FOST for a/h = 10 and for a/h = 50, it is about 12 %. As expected, the maximum displacement for a constant force applied suddenly is about twice the displacement caused by the same force applied statically (slowly).

CONCLUSIONS

1. The simple C^0 finite element formulation based on a refined shear-deformation theory is developed for transient dynamics of symmetric and unsymmetric laminates by assuming cubic variation of inplane displacements and constant variation of transverse displacement through the laminate thickness. Further, the geometric nonlinearity is incorporated using the Von Karman strains, which decreases the amplitude and period of the centre deflection and stress-resultants.

2. The evaluations using HOST show considerable warping of the transverse cross-section for composite-sandwich laminates. This true behaviour is not possible to model with a FOST. In contrast to the FOST, the present HOST does not require shear correction coefficient due to more realistic representation of the cross-sectional deformation.

3. FOST predicts significanly lower values of deflection, period, stress-resultants and stresses. As a/h ratio increases, the difference between the results of HOST and FOST decreases.

4. Finally, it is believed that the refined theory presented here is definitely an improvement over the FOST and is essential for the anisotropic composite and sandwich laminates in which the elastic properties vary drastically from layer to layer. Further their integration with the simple C^0 finite element formulation has enhanced the practical applicability of such a theoretical development. Many of the results included here can serve as references for future investigations.

ACKNOWLEDGEMENT

Partial support of this research by the Aeronautics Research and Development Board, Ministry of Defence, Government of India through its Grant No. Aero/RD-134/100/84-85/362 is gratefully acknowledged.

REFERENCES

Hinton, E., Rock, T. and Zienkiewicz, O.C. (1976). A Note on Mass Lumping and Related Processes in the Finite Element Method. Earthquake Engineering and Structural Dynamics, Vol.4, pp. 245-249.

Jones, R.M. (1975). Mechanics of Composite Materials. McGraw-Hill Ltd., New York.

Kant, T. (1982). Numerical Analysis of Thick Plates. Computer Methods in Applied Mechanics and Engineering, Vol. 31, pp. 1-18.

Kant, T., Owen, D.R.J. and Zienkiewicz, O.C. (1982). A Refined Higher-Order C^o Plate Bending Element. Computer and Structures, Vol. 15, pp. 177-183.

Kant, T. and Pandya, B.N. (1988). A Simple Finite Element Formulation of a Higher-Order Theory for Unsymmetrically Laminated Composite Plates. Composite Structures, Vol. 9, pp. 215-246.

Kant, T. and Mallikarjuna (1989). Transient Dynamics of Composite Plates Using 4-,8-and 9-Noded Isoparametric Elements. The International Journal of Applied Finite Element and Computer Aided Engineering - Finite Elements in Analysis and Design. (in press).

Mallikarjuna and Kant, T. (1988). On Transient Response of Laminated Composite Plates Based on a Higher-Order Theory. Proc. 3rd Intern. Conf. Recent Advances in Structural Dynamics, Southampton, U.K., Vol. I, pp. 219-228.

Mallikarjuna (1989). Refined Theories with C^o Finite Elements for Free Vibration and Transient Dynamics of Anisotropic Composite and Sandwich Plates. Ph.D. dissertation, Department of Civil Engineering, Indian Institute of Technology, Bombay, India.

Owen, D.R.J. and Hinton, E. (1980). Finite Element in Plasticity. Pineridge Press, Swansea, U.K.

Pandya, B.N. and Kant, T. (1988). Higher-Order Shear Deformable Theories for Flexure of Sandwich Plates - Finite Element Evaluations. International Journal of solids and Structures, Vol.24, pp. 1267-1286.

Tsui, T.Y. and Tong, P. (1971). Stability of Transient Solution of Moderately Thick Plates by Finite Difference Methods. AIAA Journal, Vol. 9, pp. 2062-206 2063.

Zienkiewicz, O.C. (1977). The Finite Element Method. McGraw-Hill, London.

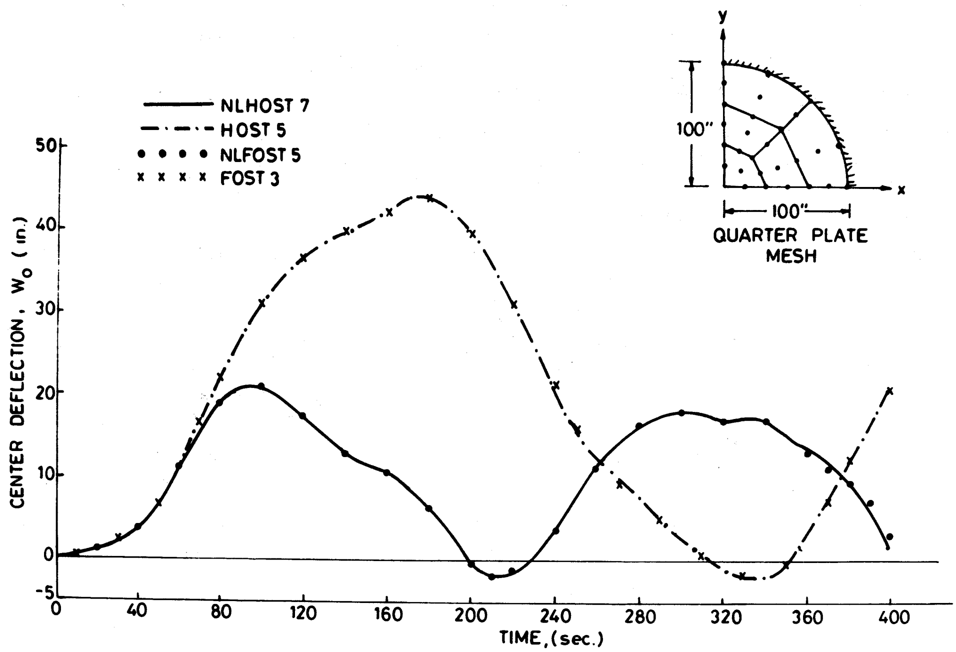

Fig. 1 Variation of centre transverse deflection versus time for a clamped circular plate (thickness = 20 inches, $q = 1.0$ lb/in^2, $\Delta t = 1.0$ sec.)

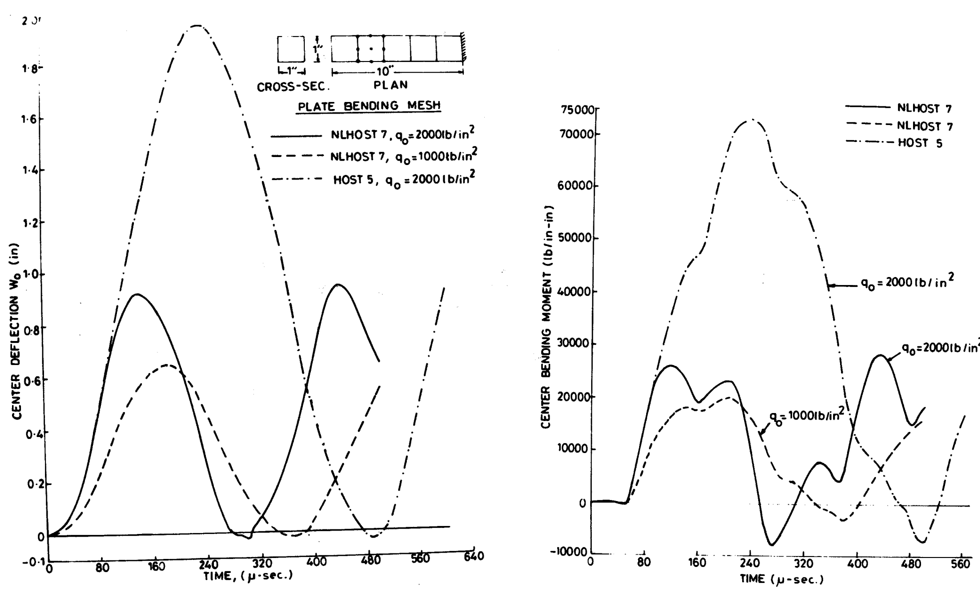

Fig. 2 Variation of transverse deflection and bending moment with time for a clamped 0^o-orthotropic plate under step load ($\Delta t = 0.5$ μ-sec)

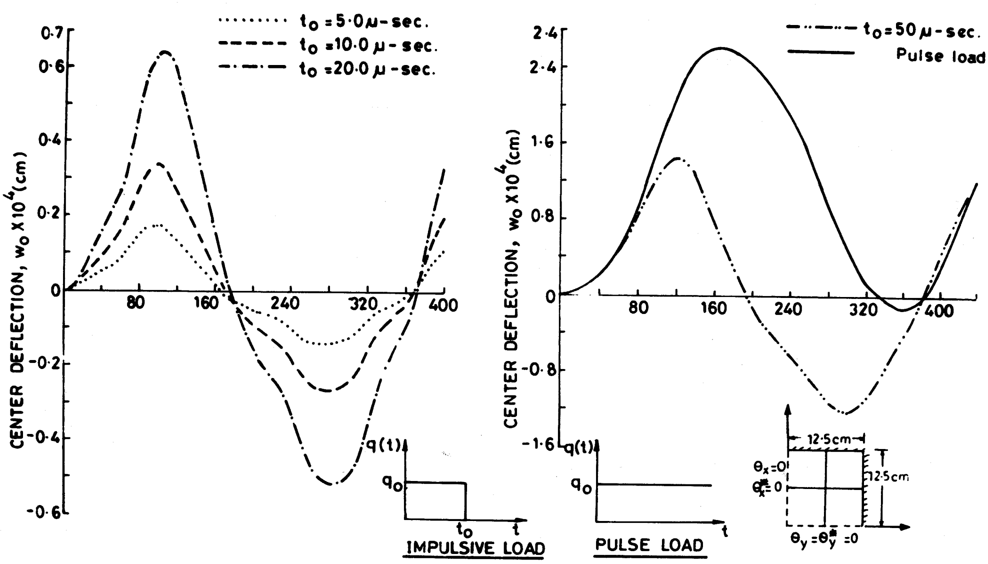

Fig. 3 Effect of impulsive loads on the transverse deflection for a symmetric laminate ($a = 25$ cm, $a/h = 10$, $\Delta t = 1.0\,\mu$-sec, $q_o = 1.0$ N/cm^2)

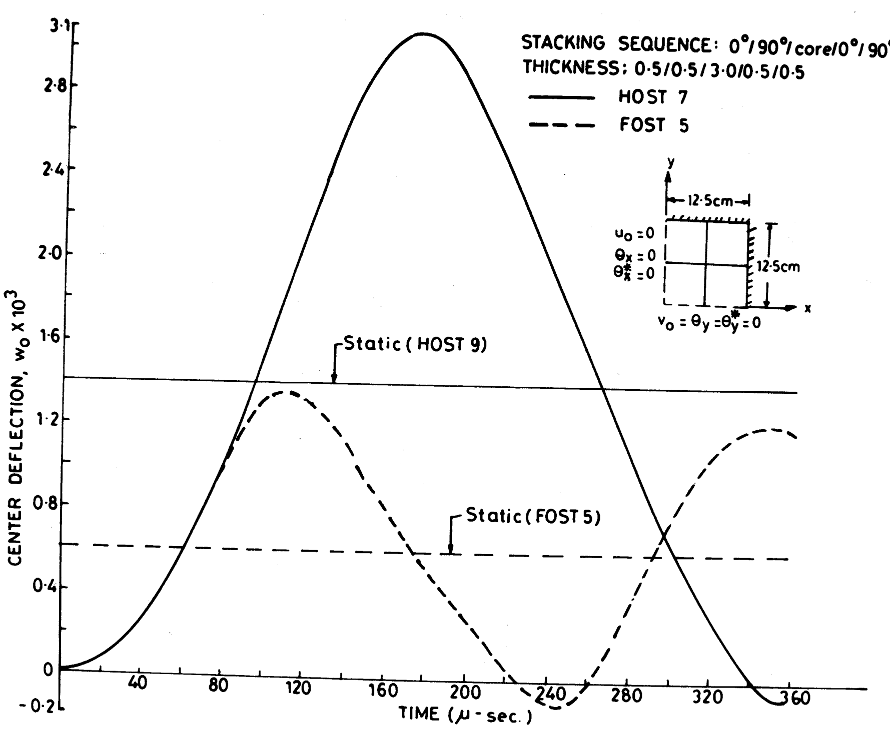

Fig. 4 Variation of transverse deflection with time for composite-sandwich plate ($a = 25$ cm, $a/h = 5$, $\Delta t = 2\,\mu$-sec, $q_o = 10$ N/cm^2)

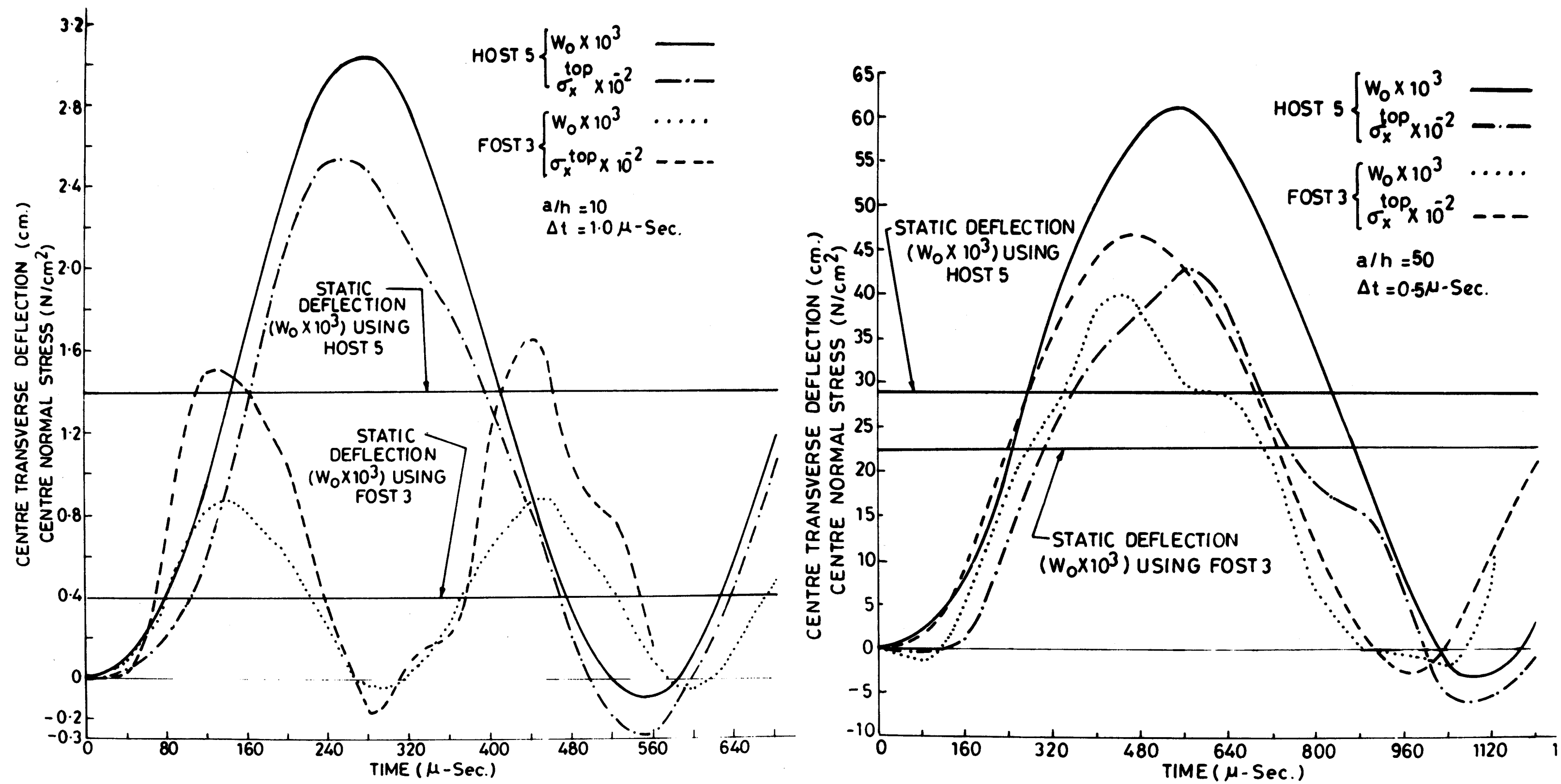

Fig. 5 Variation of deflection and normal stress for anisotropic composite-sandwich plates (Lamination scheme: $0^o/30^o/45^o/60^o$/core/$60^o/45^o/30^o/0^o$, a = b = 25 cm, q_o = 1 N/cm²)